We are IntechOpen,
the world's leading publisher of
Open Access books
Built by scientists, for scientists

6,900
Open access books available

185,000
International authors and editors

200M
Downloads

154
Countries delivered to

Our authors are among the

TOP 1%
most cited scientists

12.2%
Contributors from top 500 universities

CLARIVATE ANALYTICS

BOOK CITATION INDEX

INDEXED

WEB OF SCIENCE™

Selection of our books indexed in the Book Citation Index
in Web of Science™ Core Collection (BKCI)

Interested in publishing with us?
Contact book.department@intechopen.com

Numbers displayed above are based on latest data collected.
For more information visit www.intechopen.com

Mitigating Zinc Vapor Induced Weld Defects in Laser Welding of Galvanized High-Strength Steel by Using Different Supplementary Means

Junjie Ma, Fanrong Kong, Blair Carlson and Radovan Kovacevic

1. Introduction

Laser beam welding is a process where a focused laser beam is used as a moving heat source to join pieces of metal. The focused laser beam has a high power density that allows high speed welding, a deep penetration and a narrow heat affect zone (HAZ). There are two distinct types of laser welding modes: a conduction welding mode and a keyhole welding mode. When the laser beam intensity reaches 10^9 W/m^2, the molten pool starts to evaporate. As the laser intensity increases above 10^{10} W/m^2, the recoil pressure of the metal vapor pushes the molten metal downward and aside and a deep capillary called the "keyhole" is generated (Dawes, 1992). In the keyhole mode welding process, the keyhole maintains open due to the dynamic balance between the liquid metal surface tension and the pressure of the metal vapor and laser-induced plasma (Bakowski et al., 1984). When the laser radiates on the wall of the keyhole, the laser reflects multiple times on the wall of the keyhole. The laser beam energy is absorbed by Fresnel absorption directly by the walls of the keyhole, and a fraction of the laser energy is absorbed during each reflection (Dowden, 2009). Due to the multiple reflections of the laser beam, the keyhole behaves like an optical black body, making the keyhole mode welding process a highly energy efficient one (Steen, 2003).

Lap joint is the most common type of joint in the automotive assembly application; the traditional car body assembly method in a lap joint configuration uses resistance spot welding. However, the heavy and big spot guns limit the flexibility and accessibility of the welding process (Park et al., 2010); moreover, the localized joints are not particularly strong compared to those acquired by laser welding. On the other hand, the laser welding provides several benefits including a high scanning speed, high strength and low distortion of the joints, and the flexible implementation of the system for the automotive industry. Because of

these advantages, laser welding shows immense potential over the conventional resistance spot welding and has been widely used in the automotive industry in the fabrication of different auto bodies parts (Forrest et al., 2004).
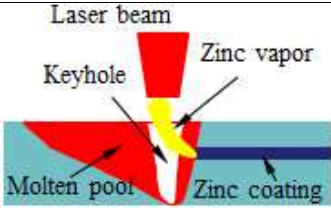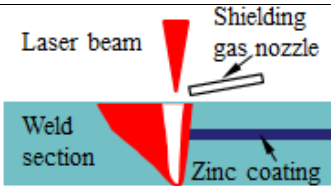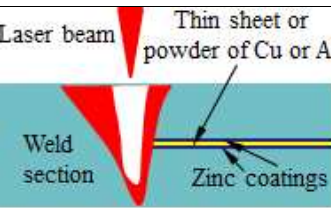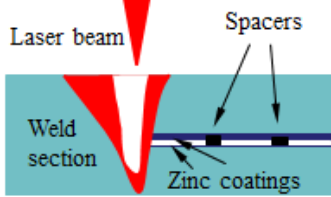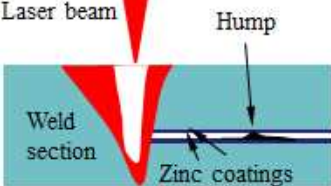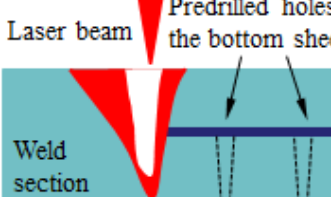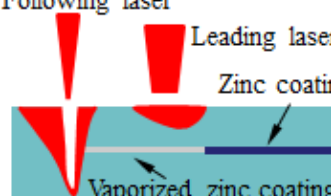
In order to reduce the weight of the vehicles and improve fuel efficiency and safety, the development of lightweight, and high-strength vehicles has prompted an increased use of advanced high strength steels (AHSS) in the automotive industry. These new steel grades include dual phase (DP) steels, transformation-induced plasticity (TRIP) steels, high hole expansion (HHE) steels, complex-phase (CP) steels, martensitic steels (MS), and twining induced plasticity (TWIP) steels (UltraLight Steel Auto Body- Advanced Vehicle Concepts, 2001). Additionally, these steels are galvanized in order to improve the surface corrosion resistance for automotive parts. However, it is still a great challenge to laser weld of galvanized steels in a zero-gap lap joint configuration. When laser welding of galvanized steels in a zero-gap lap-joint configuration, the zinc coating at the contact interface will vaporize; due to the lower boiling point (906 ºC) of zinc as compared to the melting temperature of steel (above 1500 ºC), the highly pressured zinc vapor expels the liquid metal out of the weld pool, resulting in blowholes and pores which dramatically decrease the mechanical properties of the weld (Akhter et al., 1988) (Fig. 1).
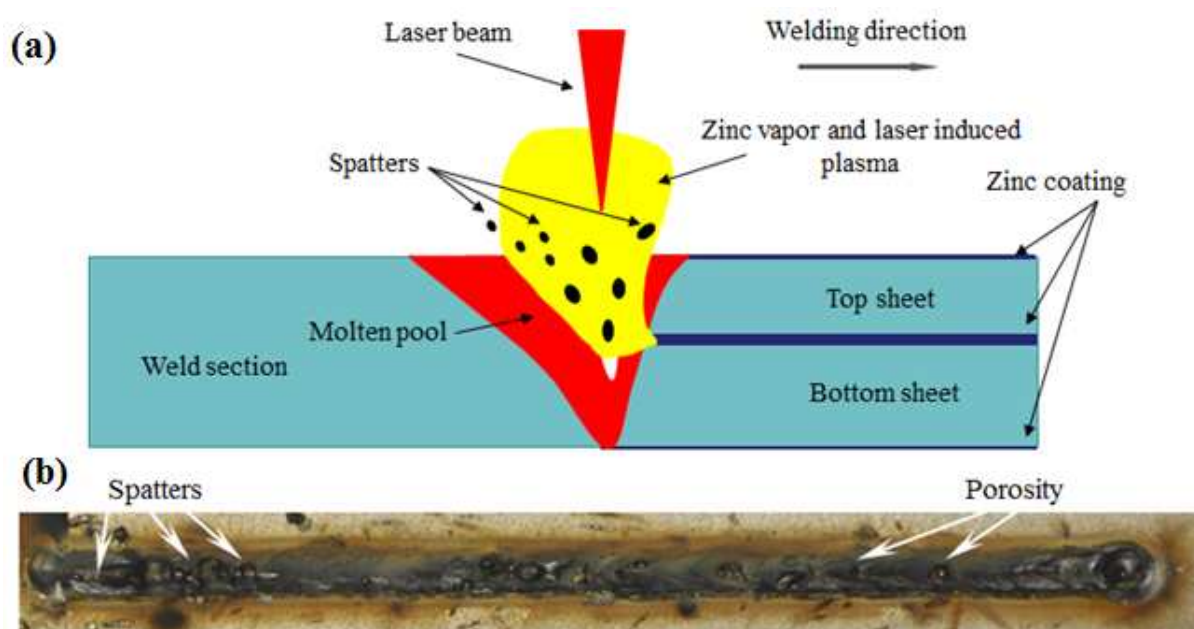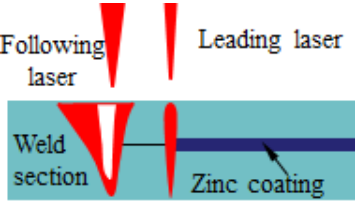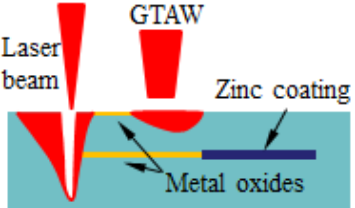
Figure 1. (a) The schematic view of the laser welding of galvanized steel in a zero gap lap-joint configuration and (b) the acquired weld bead with pores

2. Review of the laser welding of galvanized steels in a lap joint configuration

Over the past several decades, industry and academic researchers have been seeking new technologies that will successfully join galvanized steels in a lap joint configuration. Many techniques were proposed, and some are listed in Table 1.

Methods	Schematic	Technical details	Drawbacks
Elongating the laser beam (Fabbro et al., 2006) or using low power / low speed laser welding (Ma et al., 2012)		The zinc vapor was degassed through the keyhole or the enlarged molten pool during welding	
Using pulsed laser welding (Heydon et al., 1989; Kennedy et al., 1989; Norris et al., 1992; Tzeng, 1999; Tzeng, 2006)		Zinc vapor was mitigated in the pulsed laser welding and effectively exhausted through a stable keyhole	Low processing speed or unstable weld qualities that limit the application in production
Using various shielding gas combinations (Berlinger, 1987; Akhter et al., 1990; Ream, 1991; Mitsubishi Co., 1993; Chung et al., 1999; Briand et al., 2008; Yang et al., 2011)		Suppressed the formation of the laser induced zinc plasma or interacted of the zinc vapor with the shielding gas during welding	
Pre-placing a thin metal sheet or powder along the centerline of the weld seam (Dasgupta et al., 2000; Li et al., 2007)		The zinc reacted chemically with the added metal before the steel started to melt	Difficulties will be implemented in production
Applying an appropriate spacer at the faying surfaces (Akhter et al., 1988; Imhoff et al., 1988)		The generated zinc vapor vented out through the gap	
Using a laser to create humps on the bottom sheet to create a gap at the faying surfaces (Gu et al., 2011)		The generated zinc vapor vented out through the gap	The additional pre-welding procedure increases the production cost
Creating vent holes on the bottom steel sheet (Chen et al., 2009)		The generated zinc vapor vented out through the vent holes	
Adding a second laser heat source or splitting the laser beam into two laser beams in order to weld galvanized steel (Loredo et al., 2002; Xie et al., 2001)		The leading laser melted the zinc coating at the interface	Complex equipment that would be difficult to implement in the production environment.

Using a leading beam to cut a slot along the joint line (Iqbal et al., 2010; Milberg et al., 2009)		The leading laser cut the slot through which the zinc vapor was vented out	Moreover, a specific offset is needed between these two heat sources that could limit the application of this welding procedure
Applying gas tungsten arc welding (GTAW) as an auxiliary preheating heat source (Gu et al., 2001; Kim et al., 2008; Yang et al., 2009)		The preheating increased the absorption of the laser beam that contributes to a formation of a stable keyhole through which the zinc vapor is evacuated	

**Table 1.** The alternatives for the welding of galvanized steels in a lap joint configuration

As mentioned above, all of these techniques have some drawbacks that limit their application in the industry. So far, there is no report on a cost-effective, efficient, and easy-to-apply welding procedure that is capable of joining galvanized high-strength steels in a zero-gap lap joint configuration without the material addition or without the assistance of a second heat source. In order to avoid highly pressurized zinc vapor caused weld defects like spatters and blowholes, either the zinc coating should be removed before the steel melts or the vaporized zinc needs to be vented out properly during the welding process. The most direct way of accomplishing this is to mitigate the presence of high pressure zinc vapor during the welding process. In order to achieve this goal several techniques are proposed which will be described in the following sections of this chapter.

3. Low power / low speed laser welding of galvanized steels in a zero-gap lap joint configuration

3.1. Experimental procedure

Ribic et al. (2009) concluded that the generated zinc vapor escapes from the weld pool if the solidification time is longer. A lower welding speed will generate an enlarged weld pool that will require a longer solidification time. An experimental work is presented to show that the effect of zinc vapor on the quality of a weld in a zero-gap lap joint configuration may be successfully mitigated. A fiber laser of 4 kW in power with a focused spot of 0.6 mm in diameter was used as the welding heat source, and a 6-axis high precision robot was used to implement the welding procedure of galvanized steels (see Fig. 2). Pure argon with a flow rate of 30 standard cubic feet per hour (SCFH) was employed as side shielding gas to suppress the laser-induced plasma and to protect the molten material against corrosion. The base material used in this work was galvanized high strength dual phase (DP) steel DP980, whose nominal chemical composition is listed in Table 2 (Burns, 2009). The coupons of galvanized DP980 steel sheets were 1.2 mm and 1.6 mm in thickness, with a zinc coating weight of about 60 g/m^2.
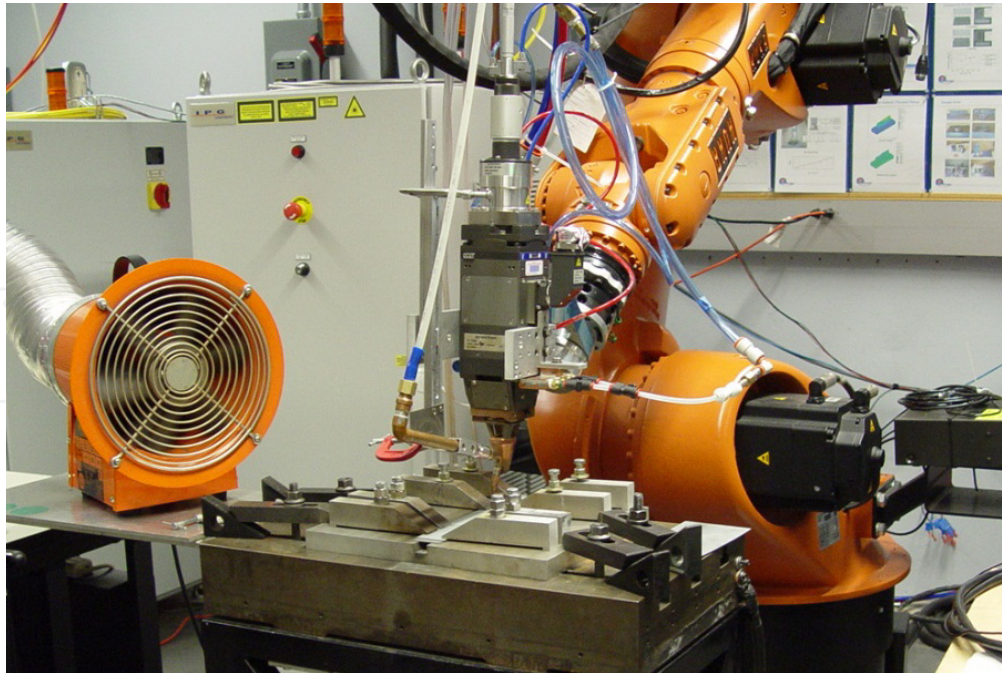
**Figure 2.** Experimental setup for low power / low speed laser welding

C	Si	Mn	Cr	Mo	Al	Cu	Ni	Fe
0.15	0.31	1.5	0.02	0.01	0.05	0.02	0.01	Balance

**Table 2.** Chemical composition of galvanized DP980 steel, wt% (Burns, 2009)

3.2. Experimental results for low power / low speed laser welding

The top and bottom views of the weld obtained under a laser power of 2.0 kW and a welding speed of 5 mm/s show an acceptable weld surface quality (see in Fig. 3). A high-speed CCD camera with a frame rate of 4000 fps combined with a green laser with a band pass filter wavelength of 532 nm as the illumination source were used for real time monitoring of the dynamic behavior of the molten pool under different laser welding conditions. The weld pool formed under a relatively low welding speed was larger and relatively stable (see Fig.4a). On the other hand, the molten pool acquired under a higher welding speed shows sever fluctuation, and the high pressured zinc vapor generated at the faying surface jetted into the molten pool causing blowholes (see Fig. 4b). According to Ribic's work, an enlarged weld pool has a longer solidification time which obviously decreased the probability that the zinc vapor would be trapped in the molten pool under a relatively low welding speed (around 5 mm/s), and a visually acceptable weld quality could be acquired. However, if the welding speed is exceedingly low, the sagging may be generated, which also reduces joint strength. Fig. 5 shows the tensile shear test results of the joints acquired under different welding speeds. A higher failure load was acquired under a lower welding speed. The trapped zinc vapor may result in pores inside the joints which could decrease the failure load with respect to the joints acquired under the same welding conditions but without zinc at the faying surface (see Fig. 5). Although an acceptable quality

of joints could be achieved by this low power / low welding speed procedure, this procedure is not accepted by the industry because of a low productivity.
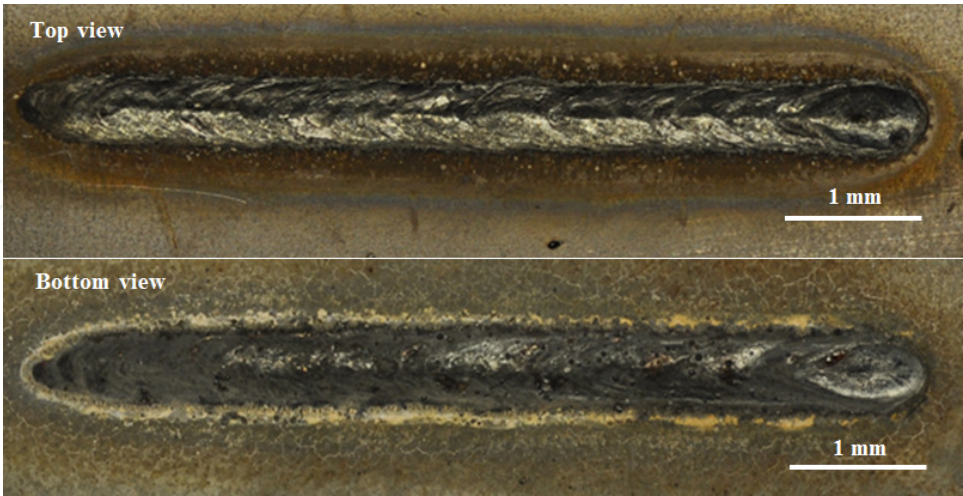
Figure 3. Top and bottom views of the weld obtained under a laser power of 2.0 kW and welding speed of 5 mm/s
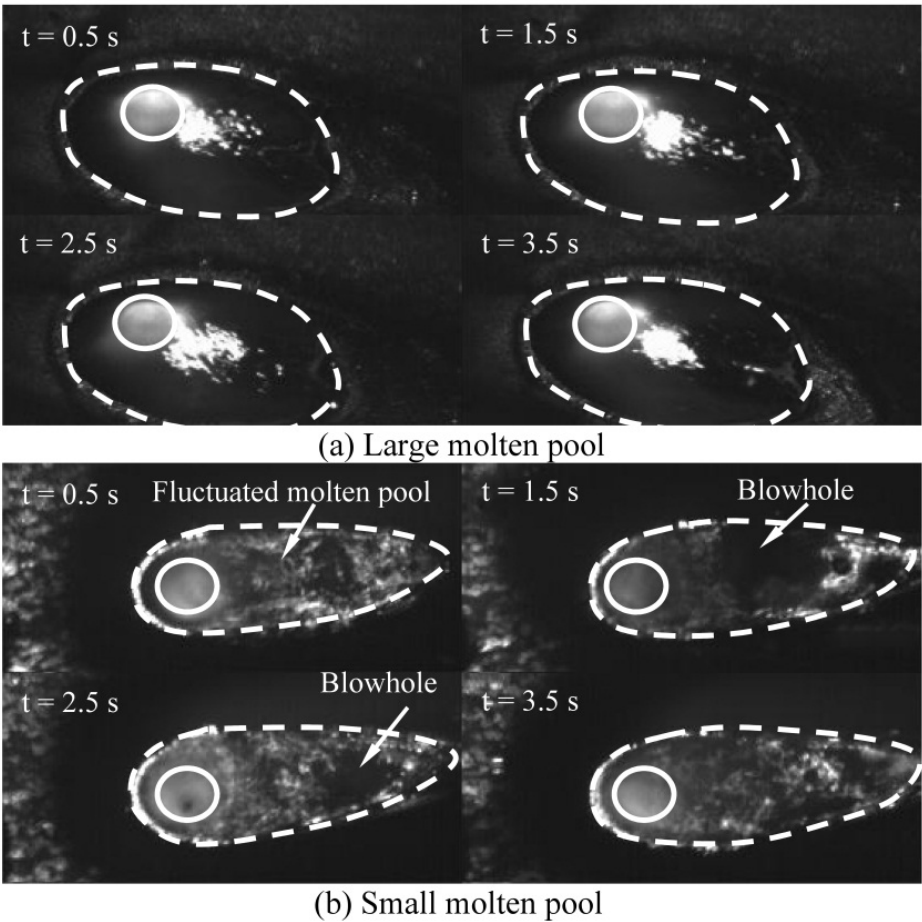
Figure 4. The dynamic behavior of the molten pool acquired under different welding parameters: (a) laser power of 1.5 kW, welding speed of 5 mm/s, and (b) laser power of 4.0 kW, welding speed of 30 mm/s at different time steps during the welding process
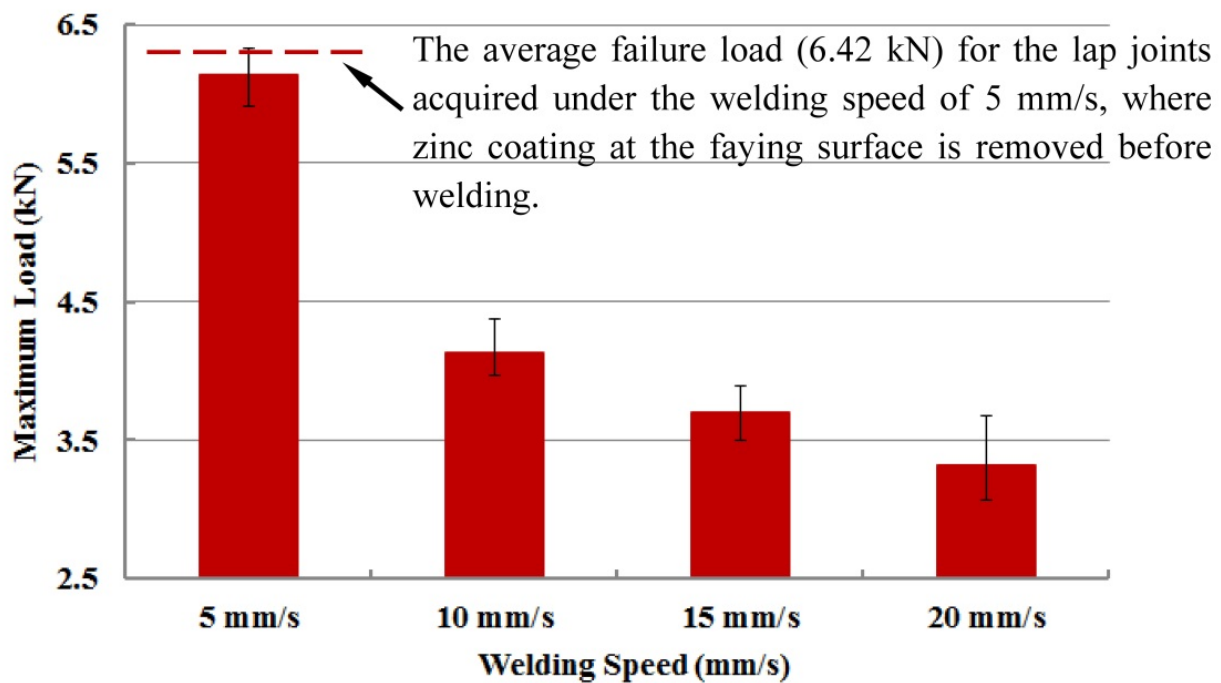
Figure 5. The failure load for tensile shear testing of the DP980 lap joints acquired under different welding speeds and with the laser power of 2.0 kW

4. Two-pass laser welding of galvanized steels in a zero-gap lap joint configuration

4.1. Experimental procedure

In order to improve the production efficiency, the automotive industry requires a welding technique that can join of overlapped galvanized high strength steels successfully under a higher working speed. As discussed previously, if the zinc coating is removed before the steel starts to melt, a much higher welding speed can be achieved. Therefore, a two-pass laser welding process that is capable of successfully joining galvanized steel sheets in a zero-gap lap joint configuration is presented. Fig. 6 shows the schematic view of the two-pass laser welding process. The defocused laser beam shown in Fig. 6a is used to preheat the two overlapped sheets during the preheating pass. Only when the width of the area where the zinc coating is vaporized by preheating is larger than the distance between the zinc boiling isotherms (906 °C), a sound weld could be acquired (see Fig. 6c). The laser power was set at its maximum value of 4.0 kW in order to allow a higher scanning speed. The laser welding speed was set at 60 mm/s in order to acquire a partial penetrated joint that was determined by the preliminary executed experimental trails. The preheating parameters, like the defocused position of the laser beam and the laser scanning speed, are critical in achieving a final weld quality. As shown in Table 3, three levels of defocused off-set distance (26 mm, 44 mm, and 62 mm which corresponds to the defocused diameters of laser beam of about 3 mm, 5 mm, and 7mm, respectively) and four levels of scanning speeds (20 mm/s, 30 mm/s, 40 mm/s, and 50 mm/s) were chosen to optimize the preheating procedure.
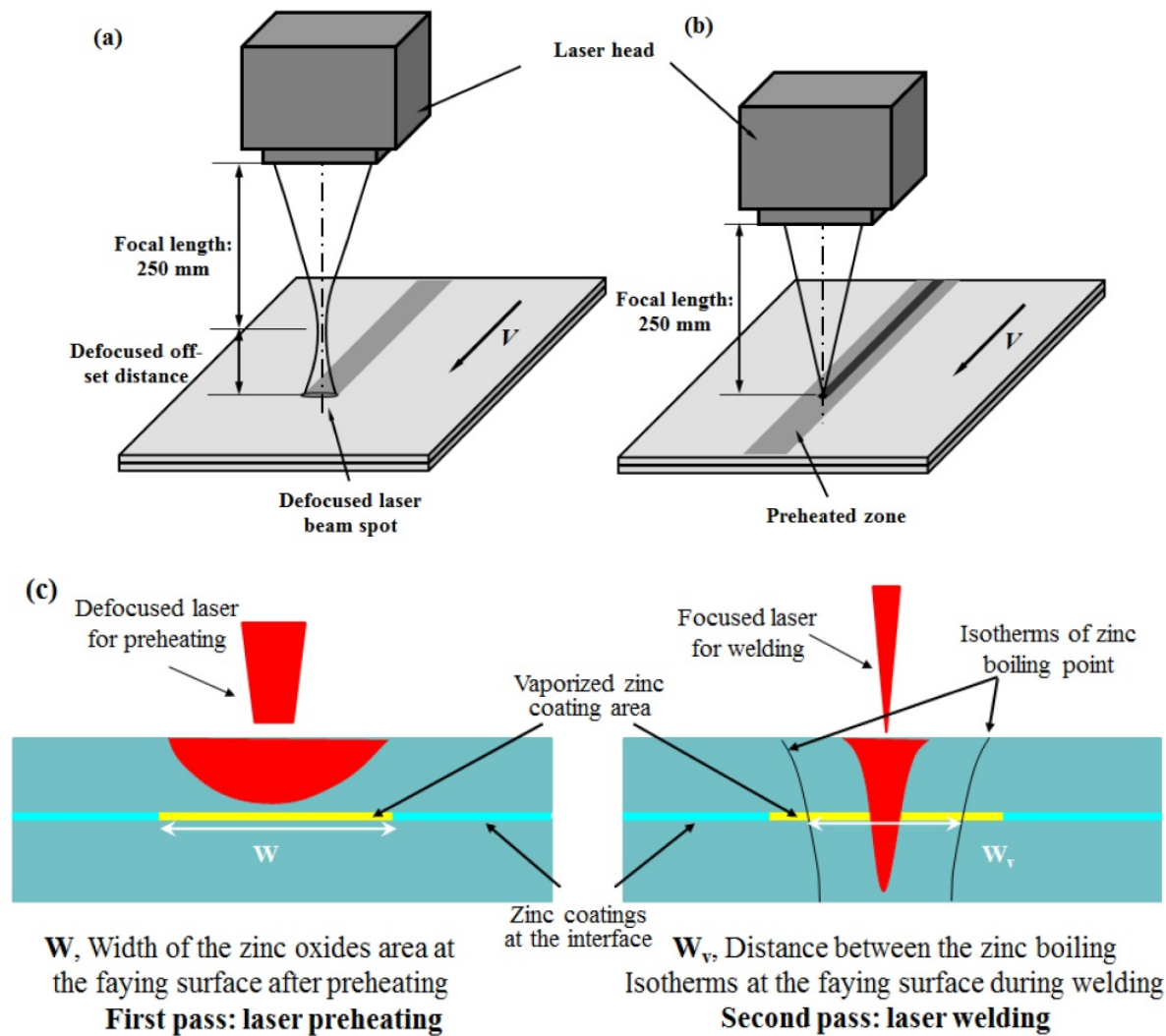
Figure 6. The schematic view of the two-pass welding process: (a) laser preheating, (b) laser welding, and (c) geometrically defined width of zinc coating treated during preheating and welding

| Process parameters	Experiment series A				Experiment series B				Experiment series C			
Scanning speed (mm/s)	20	30	40	50	20	30	40	50	20	30	40	50
Defocused off-set distance (mm)	26				44				62			

(Laser preheating and welding power: 4.0 kW, laser welding speed: 60 mm/s)

**Table 3.** The preheating parameters

4.2. Experimental results for two-pass laser welding

As the defocused off-set distance increased, the defocused laser beam spot became larger, and the laser energy distribution was dispersed. A defocused off-set distance combined with a lower scanning speed generated too much energy that penetrated the top sheet resulting

in spatters and permanent defects which could not be mitigated by the following laser welding pass (see Fig. 7a). A longer defocused off-set distance combined with a higher scanning speed could not vaporize a sufficient amount of zinc coating; the remaining zinc coating at the contact interface caused weld defects (see Fig. 7b). Thus, only for the optimized laser defocused off-set distance and the scanning speed, will a reasonable width of the zinc coating be vaporized (see Fig. 7c). Fig. 8 shows the experimental results for the selected preheating parameters (shown in Table. 3). The optimized preheating parameters that allowed a sound weld are shown in Fig. 8, area A.
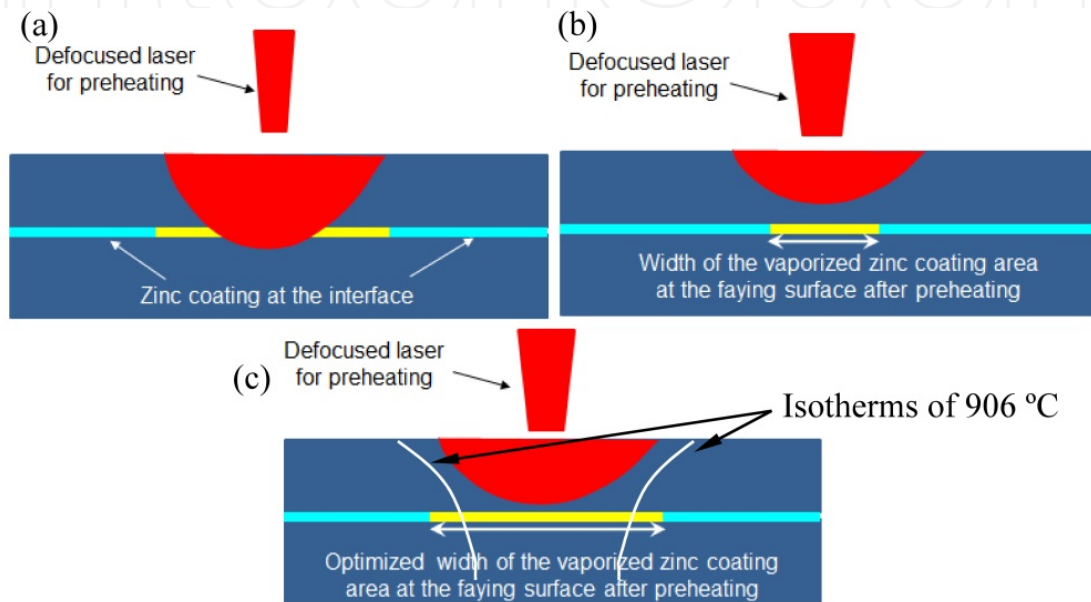

Figure 7. The schematic view of the preheating process: (a) molten pool penetrates the interface, (b) narrow vaporized zinc coating area, and (c) optimized width of the vaporized zinc coating area
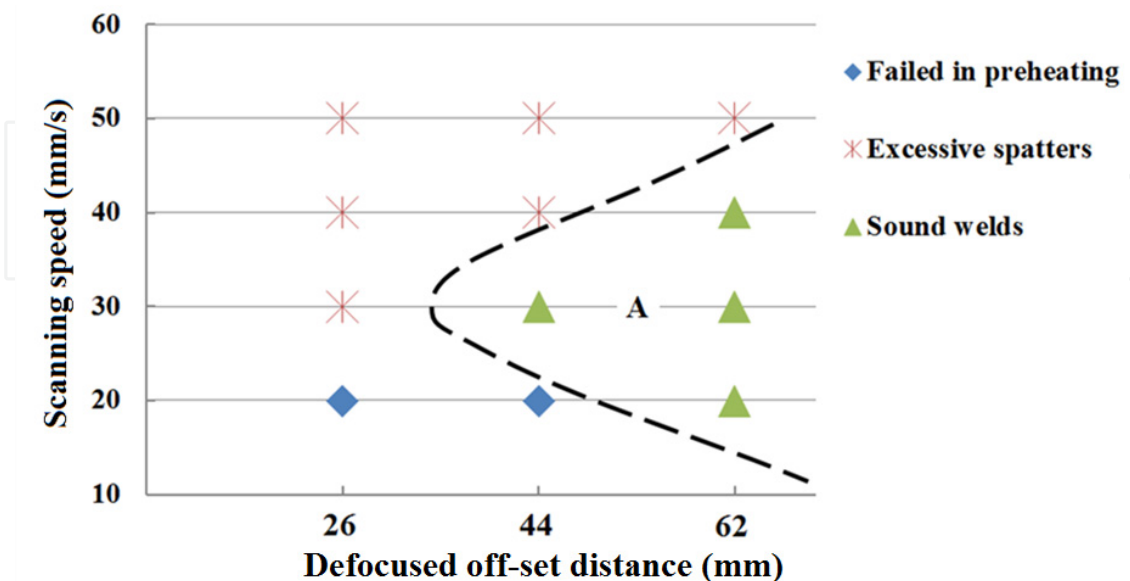
Figure 8. Experimentally determined combinations of defocused off-set distance and scanning speed that result in a good weld quality

Figs. 9 and 10 show the preheated interfaces of the coupons and the cross-sections corresponding to the different locations marked on the preheated interfaces. The zinc coatings far from the preheated zones at the top and bottom sheets are not affected (see Figs. 9b and 10b); the zinc coatings are melted and deformed at the edges of the preheated zone (see Figs. 9c and 10c); and the zinc coatings are vaporized at the center of the preheated zone (see Figs. 9d and 10d).
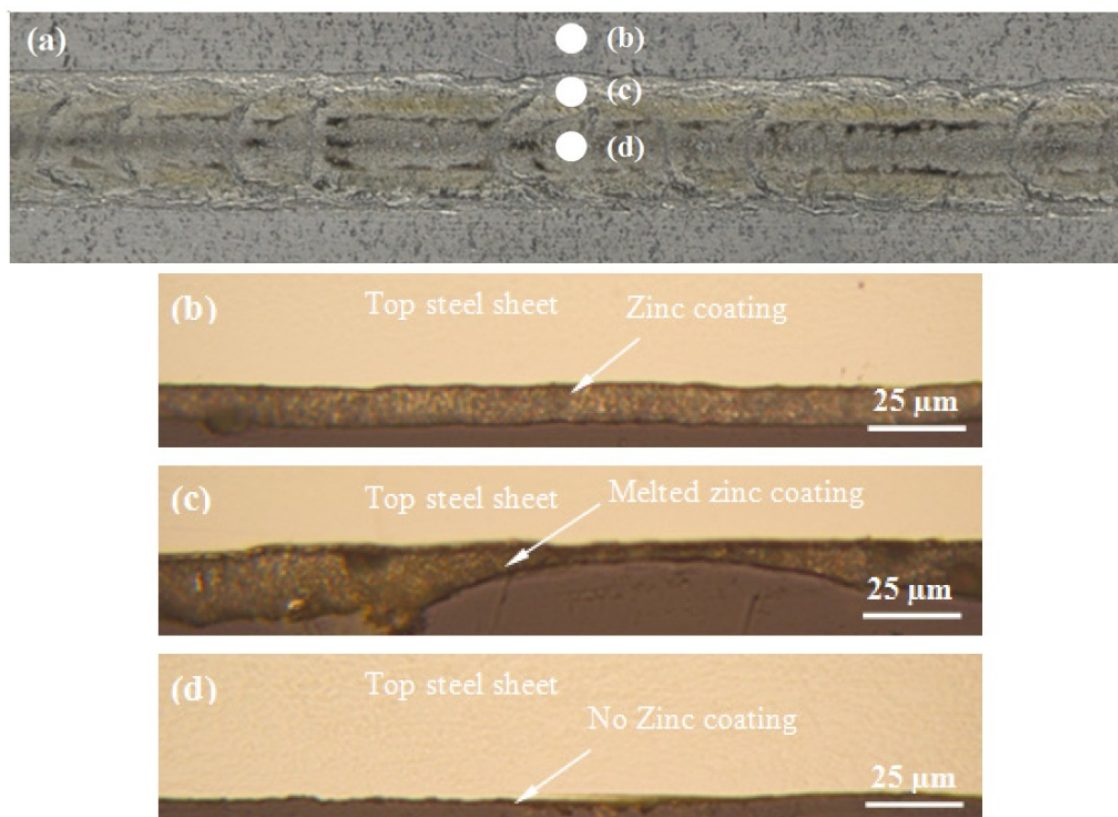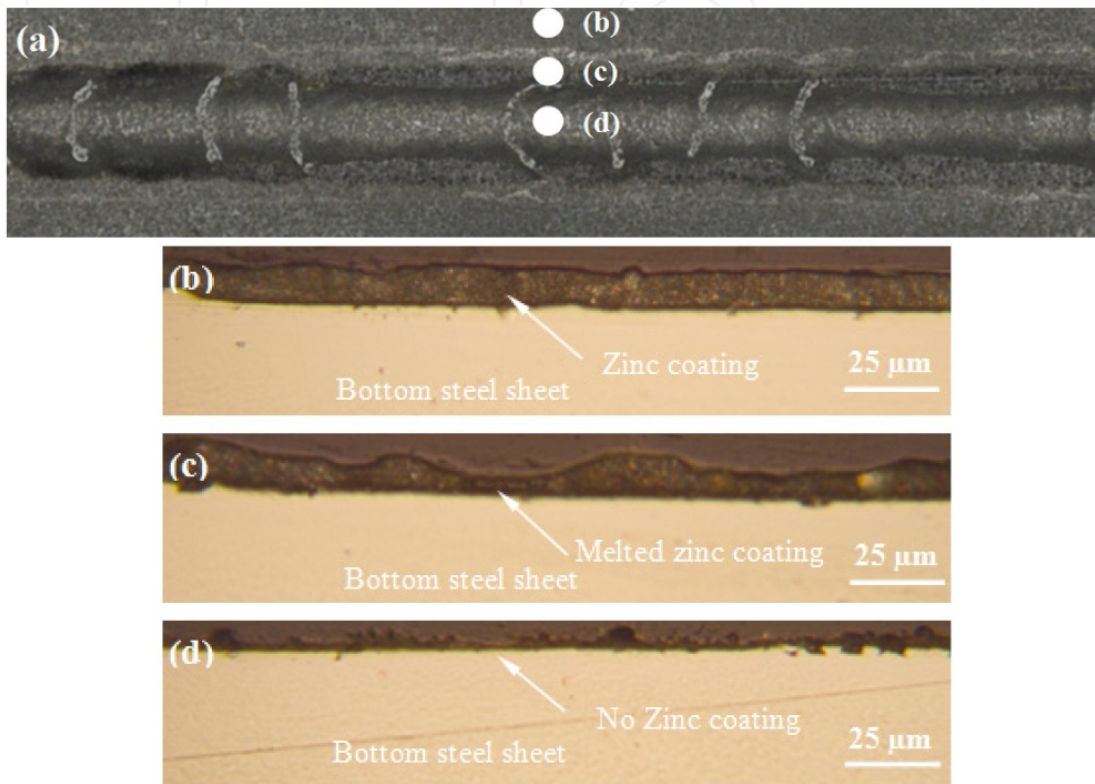

Figure 9. Preheated surface of the top steel sheet obtained with a laser power of 4.0 kW, a 30 mm/s scanning speed, and a 62 mm defocused laser beam off-set distance and the corresponding cross-section at different locations

During the laser preheating pass, the defocused laser beam burns the zinc at the top surface, and melts and partially vaporizes the zinc coatings at the interface of the two overlapped steel sheets, and improves the absorption of the laser beam which results in the formation of a stable keyhole through which any zinc vapor formed at the interface will be vented out (Yang et al., 2009). Fig. 11 shows the top and bottom views of the weld obtained under preheating and welding with a laser power of 4.0 kW, a defocused off-set distance of 62 mm, a scanning speed of 30 mm/s, and a welding speed of 60 mm/s. Fig. 12 shows the weld cross-section of the weld shown in Fig. 11.

The tensile shear test was carried out in order to determine the mechanical strength of the welded joints obtained by the two-pass laser welding procedure. The experimental results demonstrated that the two-pass welded joints were broken in the HAZ of the bottom steel sheet. One of the tensile shear results is shown in Fig. 13. The tensile shear test for the

welded coupons without a zinc coating at the interface was also performed. In order to use the data as a reference, the welded coupons without a zinc coating at the interface had a average failure load value of 5295.88 N which was lower than that of the two-pass welded coupons (6127.58 N). The reason for this difference in results is explained by the fact that the preheating process increased the laser beam absorption of the coupons, which contributed to a stronger (wider) partially penetrated weld joint.

Figure 10. Preheated surface of the bottom steel sheet obtained with a laser power of 4.0 kW, a 30 mm/s scanning speed, and a 62 mm defocused laser beam off-set distance and the corresponding cross-section at different locations
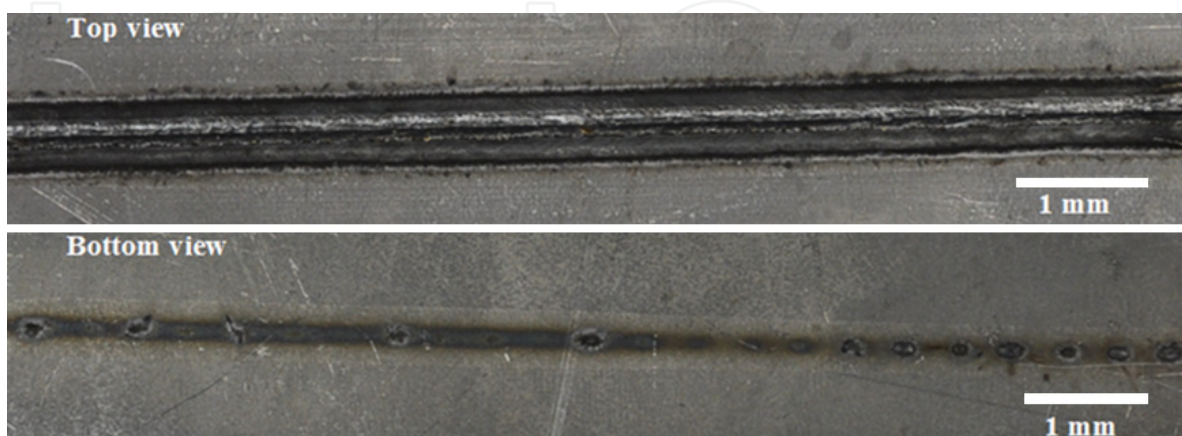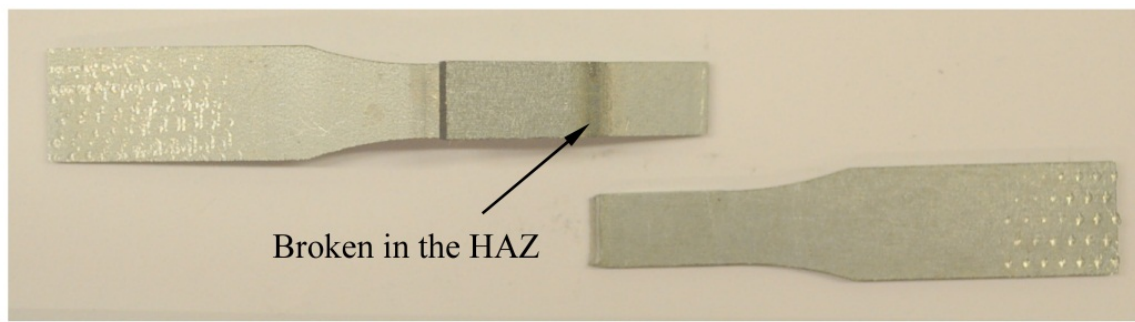

Figure 11. Top and bottom views of weld obtained under a scanning speed of 30 mm/s and a defocused off-set distance of 62 mm (the preheating and welding laser power is 4.0 kW; the welding speed is 60 mm/s)
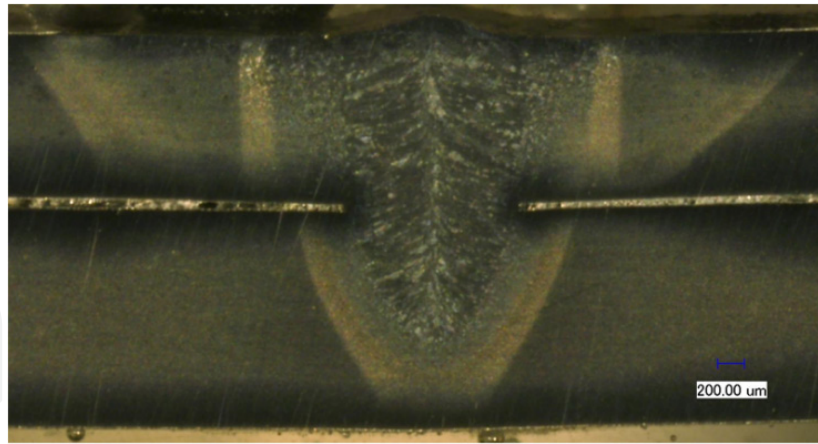
Figure 12. Cross-sectional view of the weld obtained under a scanning speed of 30 mm/s and a defocused off-set distance of 62 mm (the preheating and welding laser power is 4.0 kW; the welding speed is 60 mm/s)


Broken in the HAZ

Figure 13. Tensile shear test results of the weld joint obtained under a scanning speed of 30 mm/s, and a defocused laser beam off-set distance of 44 mm (the preheating and welding laser power is 4.0 kW; the welding speed is 60 mm/s)

5. Laser welding of galvanized steels in a lap joint configuration with a pressure wheel

5.1. Experimental procedure

Based on the experimental study performed, it was found that the stability of the laser welding process was sensitive to the clamping conditions. A relatively loose clamp condition resulted in a better weld than a very tight clamp condition. The gap ahead of the weld pool is the key to performing the laser welding of galvanized steel in a lap joint configuration successfully. Moeckel et al. (2003) developed a device for controlling the gap at the faying surface of the overlapped galvanized steel sheets in order to degas the generated zinc vapor during the welding process. The Fraunhofer Institute developed a pressure wheel system which could control the roller clamping force that allows for the controlling of the gap at the faying surface (Fraunhofer Institute website). In order to achieve an over lapped galvanized steel joint with a single laser beam without a pre- and/or post-weld process, a force-controllable pressure wheel (ZM YW50 PW P300 II) is used to control the gap near the laser focused spot during the laser welding. The laser welding of

galvanized steels for a lap joint configuration with a pressure wheel control system is shown in Fig. 14. Fig. 15a shows the close-up of the pressure wheel set-up. The laser head is set-up under a 30 °decline with respect to the pressure wheel, and Fig. 15b shows the pressure wheel controller.
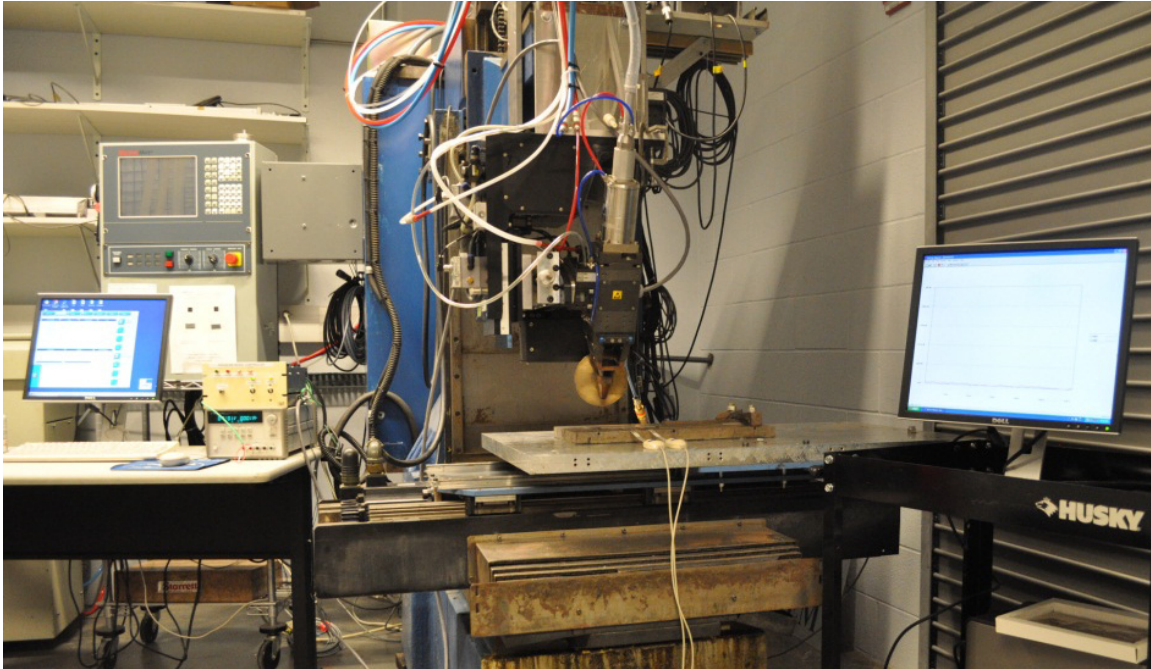
Figure 14. Laser welding of galvanized steel for a lap joint configuration with a pressure wheel control system
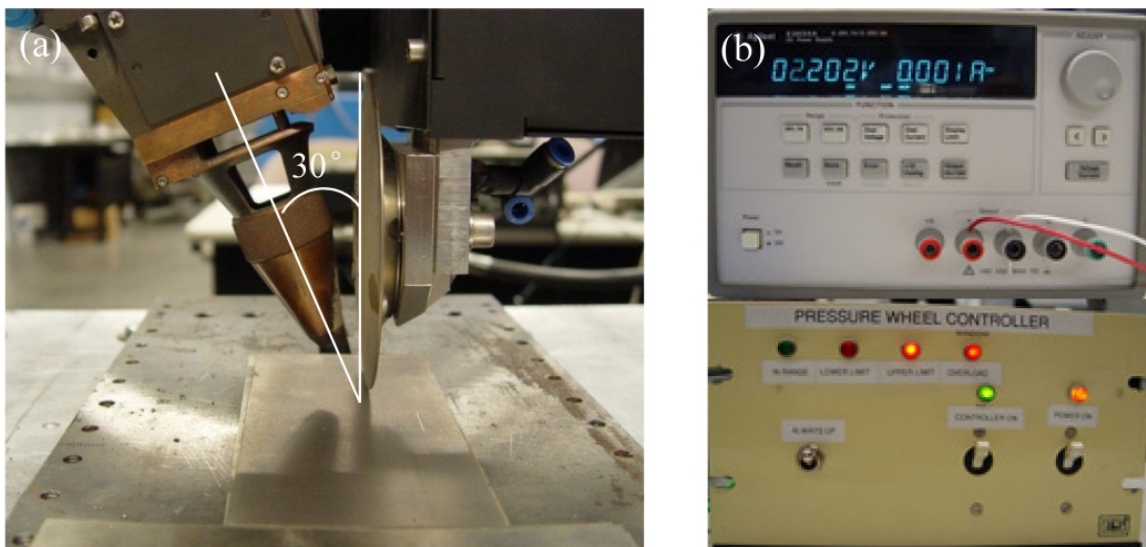

Figure 15. (a) The close-up of pressure wheel set-up and (b) the pressure wheel controller

5.2. Experimental results for laser welding with a pressure wheel

The feasibility of welding galvanized steel sheets in a lap joint configuration by controlling the pressure wheel force during the fiber laser welding process is discussed. Fig. 16 shows

the welds obtained by various levels of pressure wheel force under a laser power of 4.0 kW and a welding speed of 50 mm/s. The corresponding weld cross-sections are shown in Fig. 17. The cross-sections of the welds show that the weld beads are under the angle because the laser head is set-up with an angle of 30° with respect to the pressure wheel (see Fig. 15a). A sound weld was obtained by using a single laser beam with a force-controllable pressure wheel under the optimized force. As shown in Figs. 16 and 17, with an increased pressure wheel force, the weld quality decreased, and lots of spatters and blowholes were generated (see Fig. 16d). An increased pressure wheel force larger than 12N resulted in a decreased gap between the overlapped sheets near the laser focused area; the gap became too narrow to evacuate the generated high pressured zinc vapor. The jet of high pressured zinc vapor generated spatters and blowholes during the welding process.
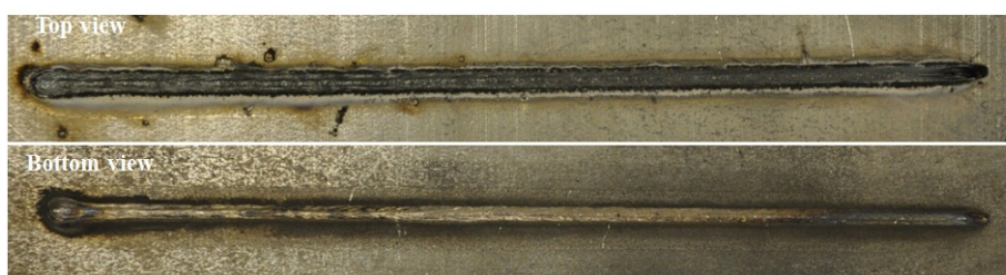
(a) Top and bottom views of the weld acquired under a pressure wheel force of 0.3 N
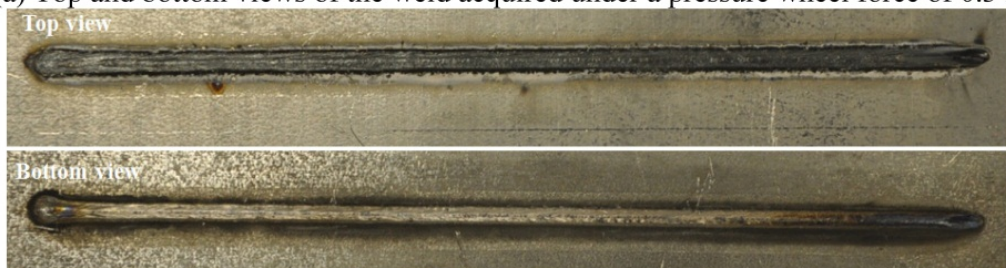
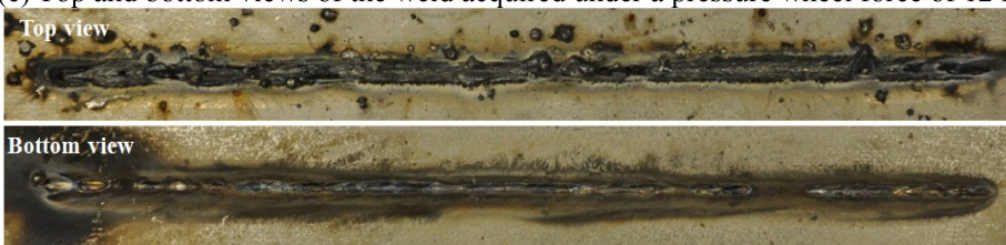(b) Top and bottom views of the weld acquired under a pressure wheel force of 6 N
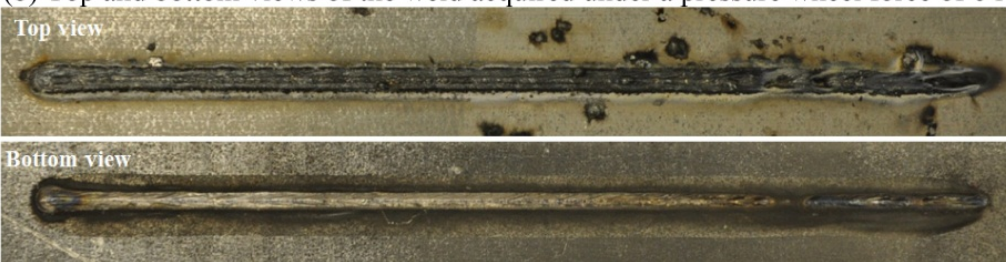
(c) Top and bottom views of the weld acquired under a pressure wheel force of 12 N

(d) Top and bottom views of the weld acquired under a pressure wheel force of 18 N

Figure 16. Top and bottom views of the welds acquired by various pressure wheel forces under a laser power of 4.0 kW and a welding speed of 50 mm/s

(a) Pressure wheel force of 0.3 N   (b) Pressure wheel force of 6 N

(c) Pressure wheel force of 12 N   (d) Pressure wheel force of 18 N
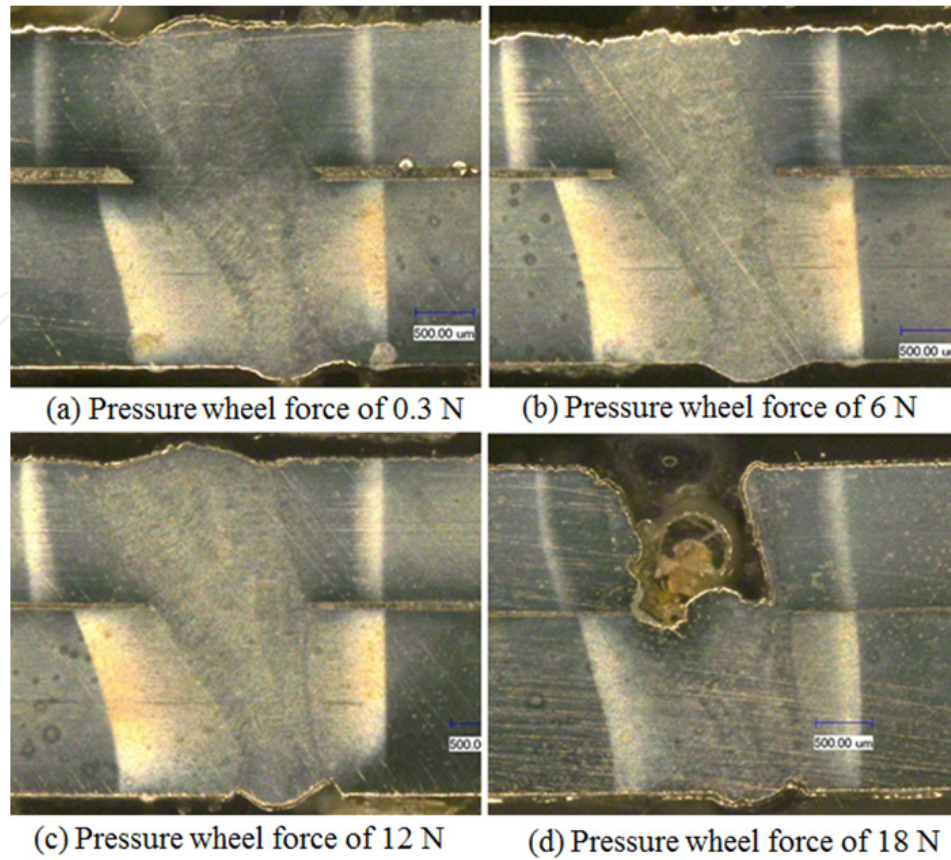
Figure 17. Cross-sectional views of the welds acquired by various pressure wheel forces under a laser power of 4.0 kW and a welding speed of 50 mm/s

Kong et al. (2012) reported that there is a correlation between the optical emission of the plasma and zinc vapor induced welding defects in the laser welding of galvanized steel for an overlapped joint configuration. Therefore, the spectroscopy was used to on-line monitor the laser welding of galvanized steel with a pressure wheel for an overlap joint configuration. The set-up to monitor the optical emission of the plasma in laser welding is shown in Fig. 18.

The emission line intensities detected from plasma during the laser welding of galvanized steel under various pressure wheel forces are shown in Fig. 19. The intensities of the emission lines above the weld pool were much lower when the pressure wheel force is larger than 12 N; while, the intensities of the emission lines were relatively higher when the pressure wheel force is set at 0.3, 6 or 12 N. The reason for this stems from the fact that when welding of galvanized steel under a higher pressure wheel force (18 N), the gap near the focal laser spot became too narrow to evacuate the high pressured zinc vapor; the zinc vapor caused spatters that disturbed the stability of the plasma which affected the intensity of the detected spectrum (Kong et al. 2012). The evolution of iron electron temperature within the laser-induced plasma along the weld bead length is shown in Fig. 20. The iron electron temperature was calculated by using the Boltzmann Plot method expressed by Equation (1) (Kong et al., 2012, Griem, 1997 and Marotta, 1994):
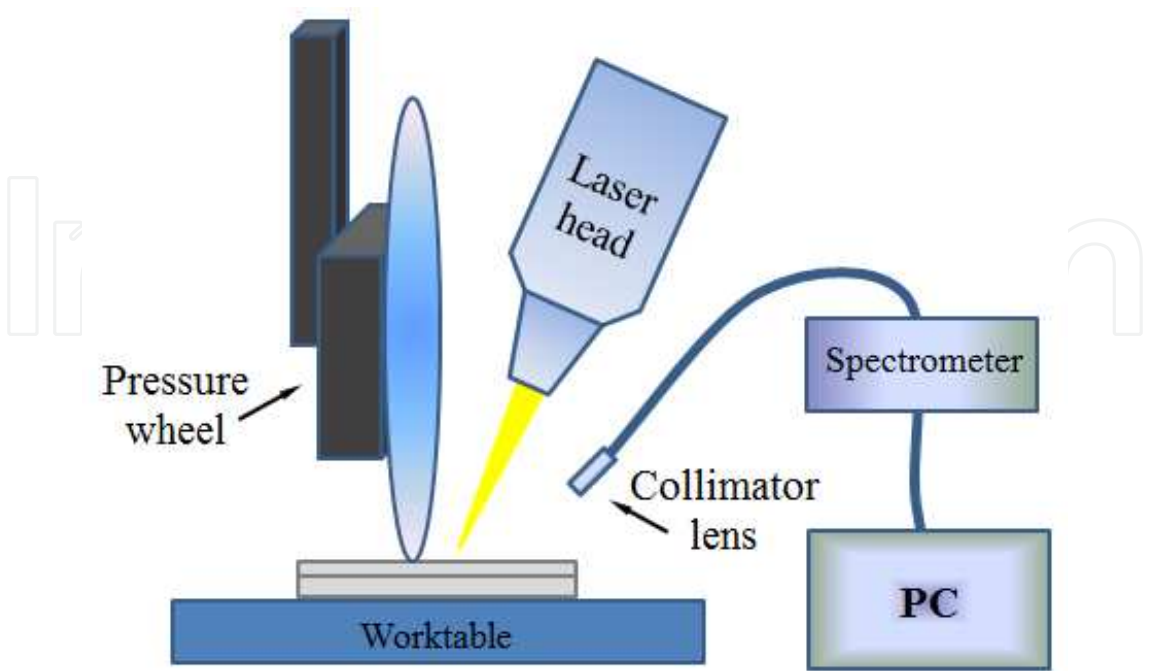
Figure 18. Schematic view of the setup for on-line monitoring the optical properties of plasmas during laser welding

(a) Pressure wheel force of 0.3 N

(b) Pressure wheel force of 6 N

(c) Pressure wheel force of 12 N
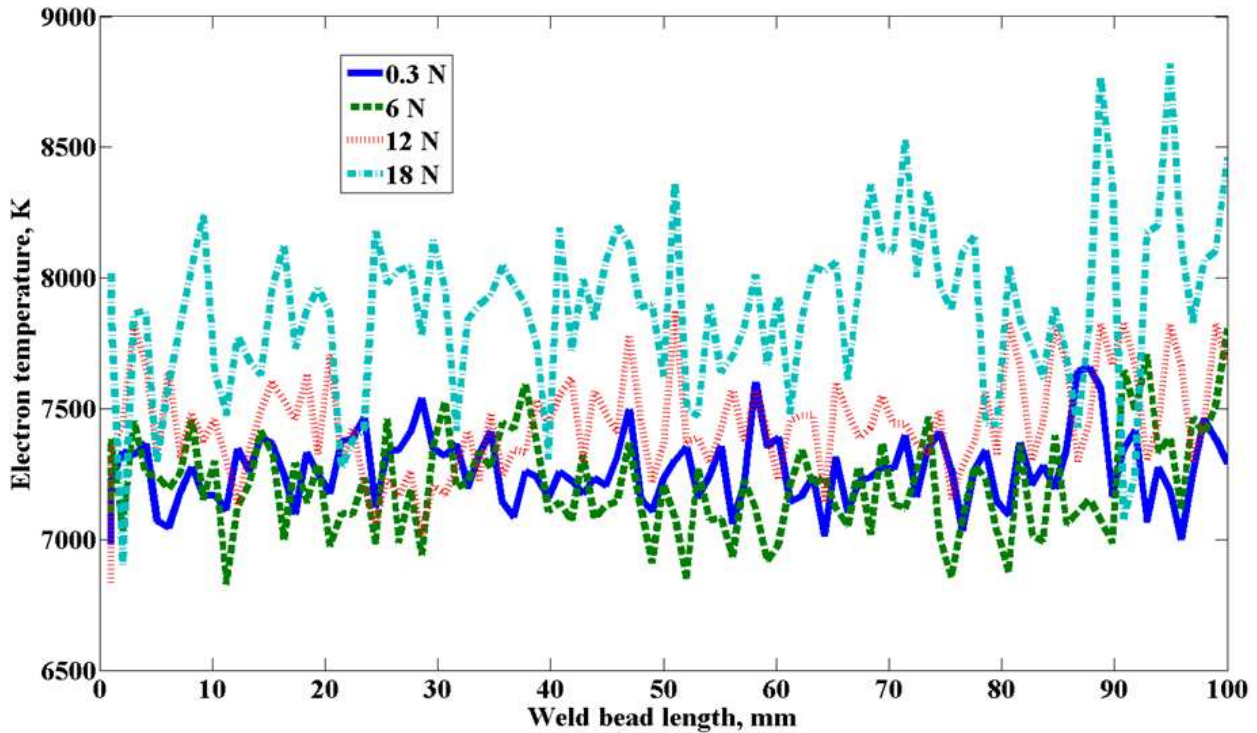
(d) Pressure wheel force of 18 N
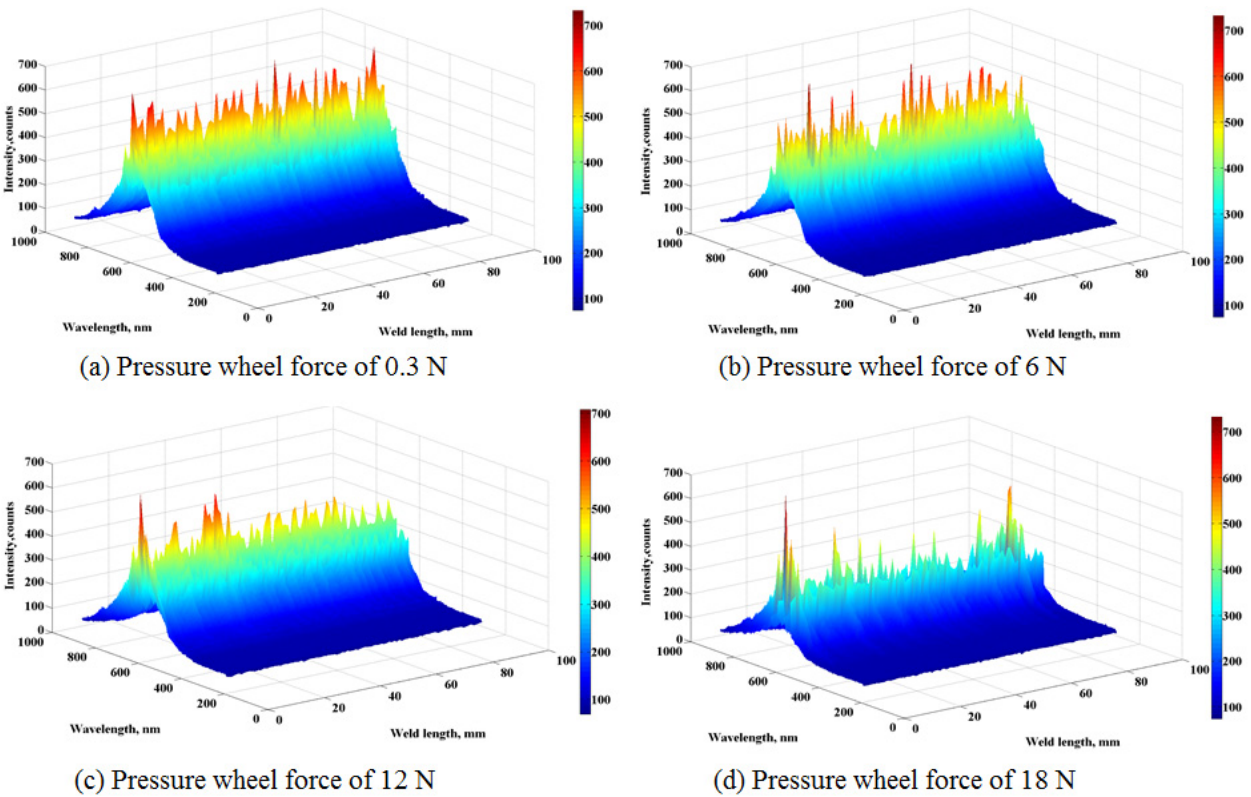
Figure 19. Spectrum of laser induced plasma captured by a spectrometer in the laser welding process by various pressure wheel forces under a laser power of 4.0 kW and a welding speed of 50 mm/s

$$T_e = \frac{E_m(2) - E_m(1)}{k\ln\left[\dfrac{E_m(1)I(1)A_m(2)g_m(2)\lambda(1)}{E_m(2)I(2)A_m(1)g_m(1)\lambda(2)}\right]} \tag{1}$$

where T_e is the plasma electron temperature, E_m is the energy of the upper state, k is the Boltzmann constant, I_m is the emission line relative intensity, A_m is the transition probability, g_m is the statistical weight, and λ_m is the wavelength.

As shown in Fig. 20, under lower pressure wheel forces (0.3, 6, and 12 N), the electron temperature showed lower intensity and less fluctuation compared to a higher pressure wheel force (18 N). The presence of the zinc vapor induced spatters in the plasma which increased the iron electron concentration which, in turn, increased the iron electron temperature value (Kong et al., 2012).

Thus, there is a correlation between the optical emission of the plasma and zinc vapor induced welding defects during the laser welding; and this optical signal could be further used as feedback for the closed-loop control of the laser welding of galvanized steel with a pressure wheel, which is shown in Fig. 21.

Figure 20. Electron temperatures of iron in laser-induced plasma captured by a spectrometer in the laser welding process by various pressure wheel forces under a laser power of 4.0 kW and a welding speed of 50 mm/s
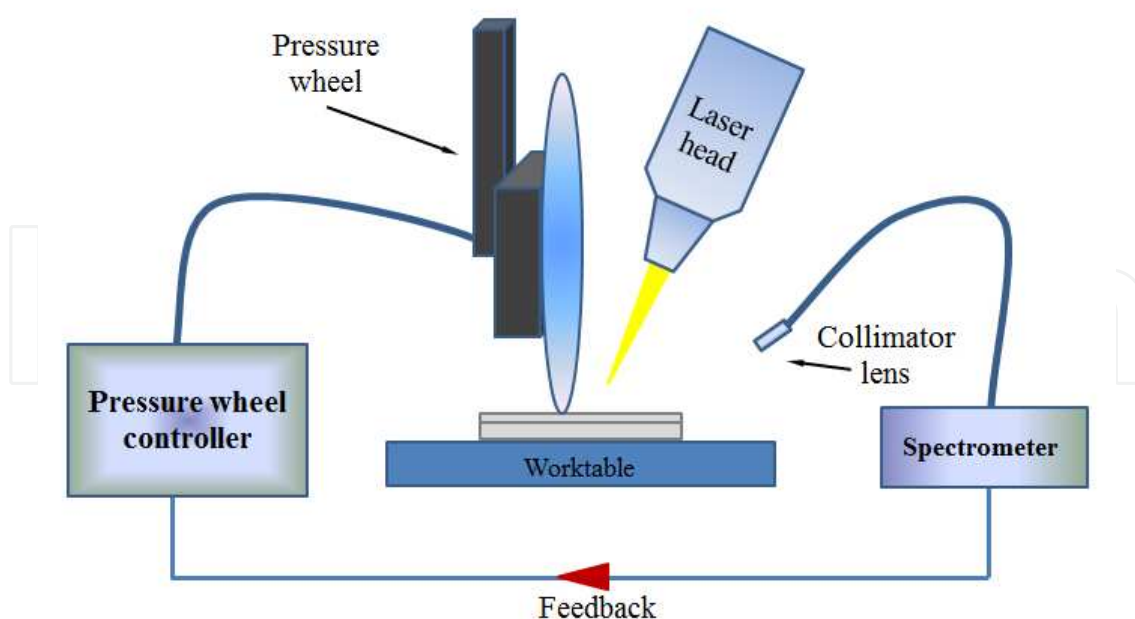
Figure 21. A schematic presentation of a closed-loop control system of the laser welding of galvanized steel by controlling the clamping force

6. Conclusions

In this chapter, issues related to the laser welding of galvanized steels in a zero-gap lap joint configuration are discussed. The authors' recent research results on the laser welding of galvanized steel in a lap joint configuration are reviewed. The different welding procedures, namely, low power / low speed welding, two-pass laser welding and laser welding with a pressure wheel are introduced for the laser welding of galvanized steels in a lap joint configuration. It was found that acceptable weld quality could be achieved by a low power / low welding speed procedure; however, the relatively low welding speed limits its application in the industrial environment. A high quality weld could be obtained by introducing a preheating pass with a defocused laser beam. By using the optical signal acquired during the laser welding process as a feedback signal in the pressure wheel force control, it is possible that a controllable clamping force could be a solution for achieving a good weld quality without using a pre- and post- welding procedure.

Author details

Junjie Ma, Fanrong Kong and Radovan Kovacevic[*]
Center for Laser-aided Manufacturing, Lyle School of Engineering, Southern Methodist University, Dallas, TX, USA

Blair Carlson
General Motors R&D Center, Warren, MI, USA

[*] Corresponding Author

Acknowledgement

7. References

Akhter R., Steen W. M. and Cruciani D. (1988). Laser welding of zinc-coated steel. Proceedings of the 5th International Conference on Lasers in Manufacturing, Stuttgart, West Germany, September 13-14

Akhter R. and Steen W.M. (1990). The gap model for welding zinc-coated steel sheet. In: Proceedings of the International Conference on Lasers Systems Application in Industry, Torino, Italy, 219-236

AWS WZC (D19.0-72), Welding Zinc-Coated Steels (1972). American Welding Society.

Bakowski L., Beyer E., Herziger G. and Poprawe R. (1984). Development and optical absorption properties of a laser induced plasma during CO_2-laser processing. SPIE Proceedings Series 455: 75-80.

Berlinger G. and Speranza J.J. (1987). U.S. Patent 4,684,779

Briand F., Chouf K. and Lefebvre P. (2008). Method and installation for laser welding with a N_2/He gas mixture, the N2/He content being controlled according to the laser power, U.S. patent 7,385,158

Burns T. Weldability of a dual-phase sheet steel by the gas metal arc welding process. Master Thesis, the University of Waterloo, 2009.

Chen W., Ackerson P. and Molian P. (2009). CO2 laser welding of galvanized steel sheets using vent holes. Materials and Design (30): 245-251

Chung B.G., Rhee S. and Lee C.H. (1999). The effect of shielding gas types on CO2 laser tailored blank weldability of low carbon automotive galvanized steel, Materials Science and Engineering 272: 357-362

Dasgupta A., Mazumder J. and Bembenk M. (2000). Alloying based laser welding of galvanized steel, Proceedings of International Conference on Applications of Lasers and Electro Optics, Dearborn MI.

Dawes C. Laser welding: a practical guide, Abington publishing, 1992.

Dowden J. M. The theory of laser materials processing: Heat and mass transfer in modern technology, Springer, 2nd edition, 2009.

Fabbro R., Coste F., Geobels D. and Kielwasser M. (2006). Study of CW Nd-Yag laser welding of Zn-coated steel sheets. Journal of physics D: Applied physics 39:401-409

Forrest M. G. and Lu F. (2004). Advanced dual beam laser welding of zinc-coated steel sheets in lap joint configuration with zero gap at the interface. 23th International Congress on Applications of Lasers and Electro-Optics, ICALEO.

Graham M. P., Hirak D. M., Kerr H. W. and Weckman D. C. (1996). Nd: YAG laser beam welding of coated sheet steels using a modified lap joint geometry. Welding Journal 75(5): 162-170

Griem H. R. Principle of plasma spectroscopy. Cambridge Monographs on Plasma Physics. Cambridge University Press, Cambridge, 1997.

Gu H. and Mueller R. (2001). Hybrid welding of galvanized steel sheet. 20th International Congress on Applications of Lasers & Electro-optics, ICALEO, 130-139

Gu H. and Shulkin B. (2011). A practical use of humping effect in laser beam welding. Journal of Laser Applications 23(1): 1-6

Gualini M.M.S., Iqbal S. and Grassi F. (2006). Modified dual-beam method for welding galvanized steel sheets in lap configuration. Journal of Laser Applications 18(185): 185-191

Heydon J., Nilsson K. and Magnusson C. (1989). Laser welding of zinc coated steel. In: Proceedings of the 6th International Conference on Lasers in Manufacturing, 93-104

Homepage Fraunhofer - Gesellschaft: Http://www.fraunhofer.de/en.html

Imhoff R., Behler K., Gatzweiler W. and Beyer E. (1988). Laser beam welding in car body making. Proceedings of the 5th International Conference on Lasers in Manufacturing, Stuttgart, West Germany, September 13-14

Iqbal S., Gualini M.M.S. and Rehman A.U. (2010). Dual beam method for laser welding of galvanized steel: Experimentation and prospects. Optics & Laser Technology 42(1): 93-98

Kim C., Choi W., Kim J. and Rhee S. (2008). Relationship between the welding ability and the process parameters for laser-TIG hybrid welding of galvanized steel sheets. Materials Transactions 49(1): 179-186

Kennedy S.C. and Norris I.M. (1989). Nd-YAG laser welding of bare and galvanized steels. SAE Technical Paper Series 890887, International Congress and Exposition, Detroit, MI

Kong F., Ma J., Carlson B. and Kovacevic R. (2012). Real-time monitoring of laser welding of galvanized high strength steel in lap joint configuration. Optics & Laser Technology 44(7): 2186-2196

Lacroix D., Jeandel G. and Boudot C. (1997). Spectroscopic characterization of laser induced plasma created during welding with a pulsed Nd: YAG laser. Journal of Physics D: Applied Physics, 81(10): 6599-6606

Li X., Lawson S. and Zhou Y. (2007). Novel technique for laser lap welding of zinc coated sheet steels. Journal of Laser Applications 19(4): 259-264

Li X., Lawson S. and Zhou Y. (2008). Lap welding of steel articles having a corrosion resisting metallic coating. U.S. Patent No. 2008/0035615 Al.

Loredo A., Martin B., Andrzejewski H. and Grevey D. (2002). Numerical support for laser welding of zinc-coated sheets process development, Applied Surface Science 195(1-4): 297-303

Ma J., Kong F. and Kovacevic R. (2012). Finite-element thermal analysis of laser welding of galvanized high-strength steel in a zero-gap lap joint configuration and its experimental verification. Materials and Design (36): 348-358

Marotta A. (1994). Determination of axial thermal plasma temperatures without Abel inversion. Journal of Physics D: Applied Physics (27): 268-272

Mazumder J., Dasgupta A. and Bembenk M. (2002). Alloy based laser welding. U.S. patent 6,479,168.

Milberg J. and Trautmann A. (2009). Defect-free joining of zinc-coated steels by bifocal hybrid laser welding. Production Engineering. Research and Development 3(1): 9-15

Mitsubishi Co. (1993). U.S. Patent 5,618,452

Moeckel A., Stein H., Jucht H., (2003). Device for degassing laser welded seams Patent no DE 10160156

Norris I., Hoult T., Peters C., Wileman P., (1992). Material processing with a 3 kW Nd:YAG laser. Proceedings of Laser Advanced Materials Processing (LAMP), Nagaoka, Japan

Pan Y. and Richardson I. M. (2011). Keyhole behavior during laser welding of zinc-coated steel. Journal of physics D: Applied physics 44:045502

Park H.S. and Choi H.W. (2010). Digital Laser Welding System for Automobile Side Panel, Laser Welding, Na, X.D., Stone (Ed.), ISBN: 978-953-307-129-9, InTech.

Ream S. (1991). Laser welding of zinc-coated steel. In: Laser applications in materials processing and manufacturing. Society of Manufacturing Engineering (SME), Southfield, MI

Ribic B., Palmer T.A. and DebRoy T. (2009). Problems and issues in laser-arc hybrid welding. Int Mater Rev 54(4):223-44

Schmidt M., Otto A., Kägeler C. (2008). Analysis of YAG laser lap-welding of zinc coated steel sheets. CIRP Annals - Manufacturing Technology, 57(1): 213-216.

Steen W. M. Laser material processing, 3rd edition, Springer, 2003.

Tzeng Y.F. (1999). Pulsed Nd:YAG laser seam welding of zinc-coated steel. Welding J 78(7): 238s-244s

Tzeng Y.F. (2006). Gap-free lap welding of zinc-coated steel using pulsed CO2 laser. The International Journal of Advanced Manufacturing Technology, (29)3-4: 287-295

ULSAB-AVC Body Structure Materials, Technical Transfer Dispatch No. 6, May, 2001.

Wiese W.L. and Martin G.A. Wavelengths and transition probabilities for atoms and atomic ions. Part II. Transition Probability. 1st edition, 1980

Xie J. and Denney P. (2001). Galvanized steel welding with lasers. Welding Journal 80(6): 59-61

Yang S. and Kovacevic R. (2009). Welding of galvanized dual-phase 980 steel in a zero-gap lap joint configuration. Welding Journal 88(8): 168-178

Yang S., Carlson B. and Kovacevic R. (2011). Laser welding of high-strength galvanized steels in a zero-gap lap joint configuration under different shielding conditions. Welding Journal 90: 8s-18s